Cdc42 is required for male germline niche development in mice

AUTHOR(S):

Mori, Yoshifumi; Takashima, Seiji; Kanatsu-Shinohara, Mito; Yi, Zheng; Shinohara, Takashi

CITATION:

Mori, Yoshifumi ...[et al]. Cdc42 is required for male germline niche development in mice. Cell Reports 2021, 36(7): 109550.

ISSUE DATE:

2021-08

URL:

http://hdl.handle.net/2433/265005

Article

Cell Reports

Cdc42 is required for male germline niche development in mice

Graphical abstract

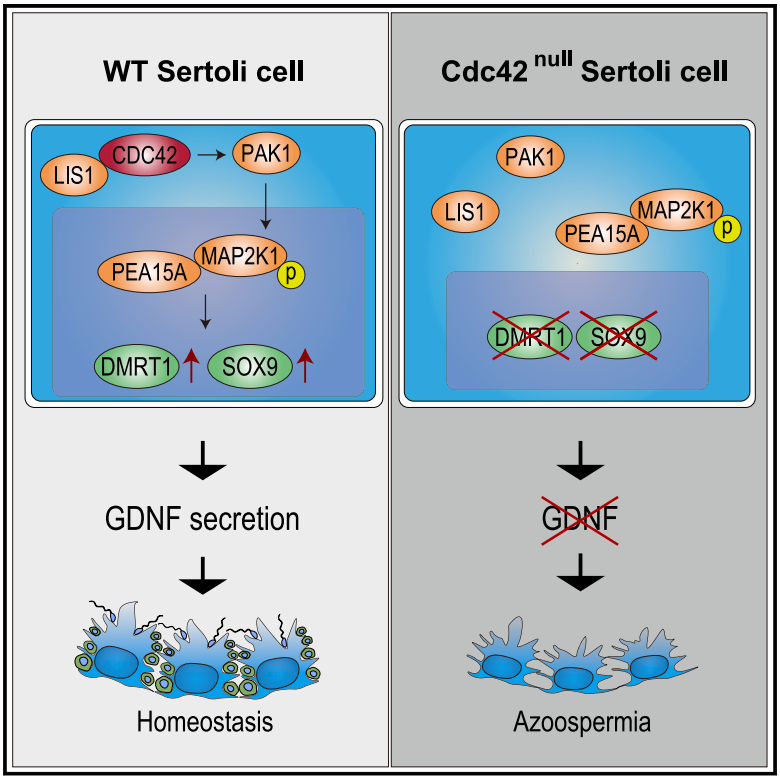

Highlights

- CDC42-deficient testes showed transient spermatogenesis and lost SSCs
- CDC42-deficient Sertoli cells exhibited weaker nuclear MAPK1/3 staining
- GDNF is downregulated in CDC42-deficient testes
- DMRT1 and SOX9 are downregulated in CDC42-deficient Sertoli cells

Authors

Yoshifumi Mori, Seiji Takashima, Mito Kanatsu-Shinohara, Zheng Yi, Takashi Shinohara

Correspondence

tshinoha@virus.kyoto-u.ac.jp

In brief

Mori et al. show that CDC42 deficiency impairs SSC niche development via downregulation of GDNF in Sertoli cells. CDC42-deficient Sertoli cells exhibit weaker nuclear MAPK1/3 staining and downregulated DMRT1 and SOX9, which suggests that the CDC42-MAPK1/3-DMRT1/SOX9 pathway plays critical roles in SSC niche development.

Mori et al., 2021, Cell Reports *36*, 109550
August 17, 2021
https://doi.org/10.1016/j.celrep.2021.109550

CellPress

Cell Reports

CellPress OPEN ACCESS

Article

Cdc42 is required for male germline niche development in mice

Yoshifumi Mori,[1,4] Seiji Takashima,[1,5] Mito Kanatsu-Shinohara,[1,2] Zheng Yi,[3] and Takashi Shinohara[1,6,*]
[1]Department of Molecular Genetics, Graduate School of Medicine, Kyoto University, Kyoto 606-8501, Japan
[2]AMED-CREST, AMED 1-7-1 Otemachi, Chiyodaku, Tokyo 100-0004, Japan
[3]Division of Experimental Hematology, Molecular Developmental Biology Graduate Program, Children's Hospital Research Foundation, University of Cincinnati, Cincinnati, OH 45229, USA
[4]Present address: Kyoen Cosmetic Surgery and Clinique, Kyoto-Karasuma, Kyoto 604-8124, Japan
[5]Present address: Department of Textile Science and Technology, Interdisciplinary Graduate School of Science and Technology, Shinshu University, Ueda 386-8567, Japan
[6]Lead contact
*Correspondence: tshinoha@virus.kyoto-u.ac.jp
https://doi.org/10.1016/j.celrep.2021.109550

SUMMARY

Spermatogonial stem cells (SSCs) are maintained in a special microenvironment called a niche. However, much is unknown about components that constitute the niche. Here, we report that *Cdc42* is essential for germline niche development. Sertoli cell-specific *Cdc42*-deficient mice showed normal premeiotic spermatogenesis. However, germ cells gradually disappeared during haploid cell formation and few germ cells remained in the mature testes. Spermatogonial transplantation experiments revealed a significant loss of SSCs in *Cdc42*-deficient testes. Moreover, *Cdc42* deficiency in Sertoli cells downregulated GDNF, a critical factor for SSC maintenance. *Cdc42*-deficient Sertoli cells also exhibited lower nuclear MAPK1/3 staining. Inhibition of MAP2K1 or depletion of *Pea15a* scaffold protein downregulated GDNF expression. A screen of transcription factors revealed that *Cdc42*-deficient Sertoli cells downregulate DMRT1 and SOX9, both of which are critical for Sertoli cell development. These results indicate that *Cdc42* is essential for niche function via MAPK1/3-dependent GDNF secretion.

INTRODUCTION

Spermatogenesis relies on spermatogonial stem cells (SSCs). SSCs continuously divide and produce progenitors throughout the life of male animals (de Rooij and Russell, 2000; Meistrich and van Beek, 1993). SSC self-renewal requires several secreted factors in a special microenvironment, called a niche. Although cellular identities of niche cells are unknown, the only somatic cell type that directly interacts with germ cells in the seminiferous tubules is Sertoli cells, which likely contribute to the maintenance of SSCs. Several cytokines are secreted from the niche, the most prominent being GDNF. Studies show that GDNF is a critical regulator of SSC self-renewal and fate. *Gdnf* heterozygous knockout (KO) mice gradually lose SSCs and become infertile, while *Gdnf* transgenic mice accumulate clumps of undifferentiated spermatogonia in the seminiferous tubules (Meng et al., 2000).

The niche is important not only for maintaining SSC self-renewal but also for attracting SSCs. SSCs microinjected into the seminiferous tubules migrate toward the niche and re-establish spermatogenesis in infertile mice (Brinster and Zimmermann, 1994). Transplanted SSCs transmigrate through the blood-testis barrier (BTB) between Sertoli cells and proliferate on the basement membrane before settling into the germline niche (Nagano et al., 1999). GDNF and CXCL12 are reportedly involved in the directed migration of SSCs (Kanatsu-Shinohara et al., 2012; Yang et al., 2013). SSCs transfected with dominant-negative *Ret*, a component of GDNF receptor, exhibited poor colonization in infertile mice upon microinjection into the seminiferous tubules. Similarly, SSCs lacking *Cxcr4*, a receptor for CXCL12, also showed reduced colonization. Although these results establish the importance of GDNF and CXCL12 in the SSC homing phenomenon, much is unknown about how these molecules are regulated in the niche to influence SSCs.

Sertoli cells are uniquely shaped cells that are significantly polarized compared with other cells. They proliferate only briefly, up to 12–14 days after birth in postnatal testes (França et al., 2016). After Sertoli cells proliferate, the BTB, which is composed of multiple tight junction proteins, is formed between adjacent Sertoli cells and divides the seminiferous tubules into basal and adluminal compartments (França et al., 2016; Mruk and Cheng, 2015; Stanton, 2016). Sertoli cells then extend numerous long, microtubule-rich processes that associate with developing germ cells to sustain spermatogenesis. Because of the unique structure of Sertoli cells and their close association with spermatogenic cells, changes in Sertoli cell morphology or activity may influence SSC homing and self-renewal. This idea is supported by our previous observation that SSCs transplanted

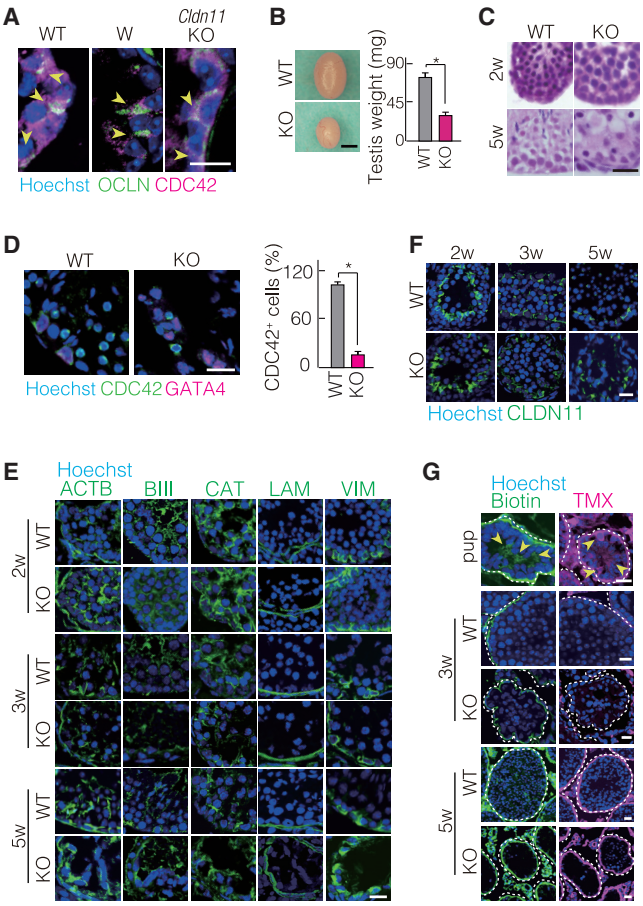

Figure 1. Characterization of Sertoli cell-specific *Cdc42*-deficient testes

(A) Immunostaining of CDC42 and OCLN in WT, W, and *Cldn11*-deficient testes. Arrowheads indicate colocalization of CDC42 and OCLN.

(B) Appearance and weight of *Cdc42*-deficient mouse testis (n = 4).

(C) Histological appearance of *Cdc42*-deficient testes.

(D) Immunostaining of CDC42 in *Cdc42*-deficient testes. Cells with CDC42 expression in GATA4^{+} cells were counted (n = 21).

(E) Immunostaining of *Cdc42* KO testes with structural protein markers.

(F) Immunostaining of CLDN11.

(G) Functional assessment of the BTB. *Cdc42*-deficient testes were injected with biotin or TMR-dextran (red) interstitially. After 30 min, the testes were fixed and sectioned. Biotin was detected by fluorescein isothiocyanate-conjugated streptavidin (green).

Arrowheads indicate dye leakage into the adluminal compartment of the seminiferous tubules. Bar, 20 μm (A), 1 mm (B), 10 μm (C), and 20 μm (D–G). Stain, hematoxylin and eosin (C), Hoechst 33342 (A and D–G). Asterisk indicates statistical significance ($p < 0.05$). See also Figure S1.

into immature testes before BTB formation generated increased colony size and area (Shinohara et al., 2001).

As a member of the Rho family small GTP-binding proteins, CDC42 is involved in various biological processes, including cell migration, signaling, and proliferation (Etienne-Manneville, 2004). Because CDC42 is important for establishing cell polarity and controlling vesicle transport, CDC42 may contribute to SSC homing or niche function. Indeed, loss of *Cdc42* in the digestive tract resulted in abnormal epithelial permeability and also resulted in increase in stem cell number and migration (Melendez et al., 2013). CDC42 is also involved in the regulation of the BTB and other tight junction structures (Erickson and Cerione, 2001; Wong et al., 2010).

Because loss of the BTB likely enhances SSC homing (Shinohara et al., 2001), we hypothesized that *Cdc42* deficiency might improve SSC transplantation efficiency. We used AMH-*Cre* transgenic mice to produce Sertoli cell-specific *Cdc42* KO mice that express the *Cre* transgene during the embryonic stage (Lécureuil et al., 2002). By using these mice and spermatogonial transplantation, we assessed the impact of *Cdc42* in Sertoli cells.

RESULTS

Deletion of Cdc42 during embryonic development

We hypothesized that deletion of *Cdc42* in Sertoli cells would improve SSC homing efficiency because CDC42 is involved in the formation of the BTB (Wong et al., 2010). We performed double immunohistochemical staining of CDC42 and the tight junction marker OCLN. CDC42 was expressed widely in the seminiferous tubules of wild-type (WT) mice testis (Figure 1A). To determine the effects of germ cells on CDC42 expression, we also examined CDC42 expression in the testes of congenitally infertile WBB6F1-Kit^{W}/Kit$^{W\text{-}v}$/J (designated W) mice, which contain only a few undifferentiated spermatogonia. In both WT and W mice, a portion of CDC42 was colocalized with OCLN, which confirmed previous findings that CDC42 colocalizes with the BTB (Wong et al., 2010). W mice showed no differences in staining pattern compared with WT mice, suggesting that germ cells do not strongly impact CDC42 cellular distribution. Because CDC42 may be regulating the BTB, we also analyzed *Cldn11* KO mice (Gow et al., 1999; Kitajiri et al., 2004), in which spermatogenesis is abrogated at the spermatocyte stage (Kanatsu-Shinohara et al., 2020). Although *Cldn11* KO mice lacked a BTB, CDC42 and OCLN were still found to colocalize (Figure 1A).

To determine the impact of *Cdc42* on Sertoli cells, we produced mice with *Cdc42*-deficient Sertoli cells by crossing *Cdc42*$^{f/f}$ mice with Amh-*Cre* transgenic mice (Lécureuil et al., 2002; Yang et al., 2007). Amh-*Cre* transgenic mice express *Cre* at around 15.5 days postcoitum (dpc) in embryonic Sertoli cells. The offspring of these crosses revealed no apparent abnormalities, and their testes contained mitotic spermatogonia at 2 weeks after birth. Sertoli cell-specific *Cdc42*-deficient mice at 3 weeks had spermatids, suggesting successful meiosis. However, their germ cells gradually disappeared thereafter, and testis size was significantly reduced by 5–8 weeks after births (Figures 1B and 1C). Immunostaining of CDC42 showed that ~80% of the Sertoli cells lacked CDC42 (Figure 1D).

We analyzed the expression of several major structural proteins to check whether *Cdc42* deficiency caused structural abnormalities in seminiferous tubules (Figure 1E; Figure S1A). Because CDC42 induces actin polymerization, we first examined distribution patterns of F-actin in *Cdc42*-deficient testes using phalloidin staining and found no apparent difference. Immunostaining also showed a normal expression pattern of intermediate filament marker VIM in *Cdc42*-deficient testes. CTNNB1

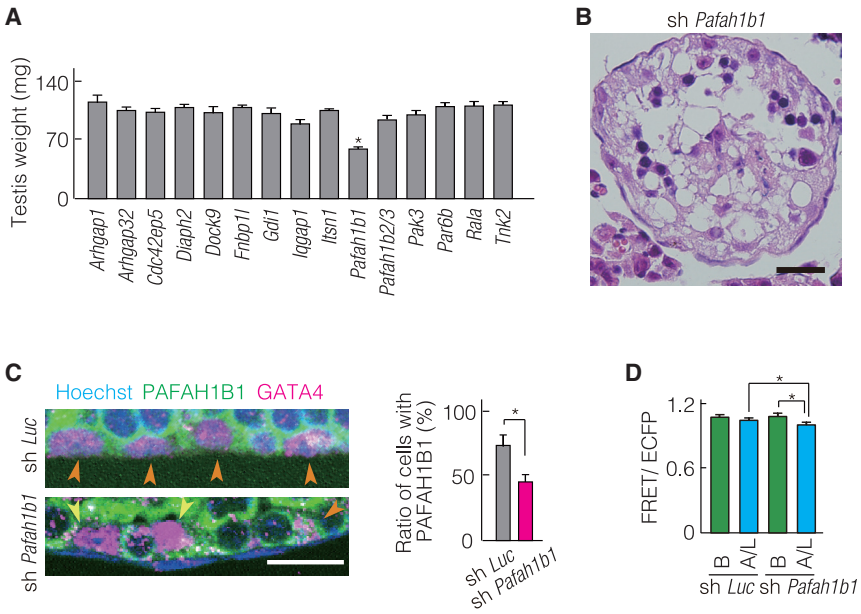

Figure 2. Functional analysis of genes regulating CDC42 activity

(A) Testis weight of WT mice that received lentiviruses expressing shRNA against the indicated genes (n = 3). Testes were recovered 5 weeks after microinjection.

(B) Histological analysis of testis that received shRNA against *Pafah1b1*.

(C) Immunostaining of PAFAH1B1 in Sertoli cells. Orange arrowheads indicate expression of PAFAH1B1 in GATA4^{+} Sertoli cells. Yellow arrowheads indicate Sertoli cells that lost PAFAH1B1 signals after shRNA transduction. A total of 18 tubules were analyzed for each sample.

(D) FRET/ECFP ratio of RaichuEV-Cdc42 probe in Sertoli cells (n > 150).

B, basal compartment; A/L, apical or lateral compartment. Asterisk indicates statistical significance ($p < 0.05$). Bar, 20 μm (B and C). Stain, hematoxylin and eosin (B), Hoecsht 33342 (C). See also Figure S2.

and TUBB3 were also stained in samples from *Cdc42*-deficient mice. CTNNB1 is reportedly involved in the regulation of Sertoli-germ cell interaction by interacting with CDC42 (Lui et al., 2005), and TUBB3 is a beta tubulin isotype uniquely expressed in Sertoli cells in an androgen-dependent manner (De Gendt et al., 2011). There were no differences in the distribution pattern of CTNNB1 or TUBB3 with *Cdc42* deficiency. Laminin distribution around Sertoli cells also did not show differences with *Cdc42* deficiency, suggesting that extracellular matrix proteins are produced and transported from Sertoli cells despite the absence of *Cdc42*.

Because the BTB is essential for completion of spermatogenesis and is regulated by CDC42 (Mruk and Cheng, 2015), we examined the expression of CLDN11, which is an essential component of the BTB (Kitajiri et al., 2004). There were no apparent changes in CLDN11 expression patterns with *Cdc42* deficiency (Figure 1F; Figure S1B). We also tested the permeability of the BTB by microinjecting biotin (557 D) or dextran (~10 kDa) into the interstitial tissues of *Cdc42*-deficient or WT mice, and found no leakage into the adluminal compartment of the seminiferous tubule (Figure 1G). On the other hand, a WT pup with underdeveloped BTB testes showed leakage into the lumen of the seminiferous tubules, which suggested that loss of CDC42 does not impair function of the BTB.

Activation of CDC42 by PAFAH1B1

To understand the mechanism of CDC42 activation, we searched for molecular regulators for CDC42 activity. We produced lentiviruses that express short hairpin RNA (shRNA) against 15 candidate genes that reportedly influenced CDC42 activities, including *Arhgap1*, *Arhgap32*, *Cdc42ep5*, *Diaph2*, *Dock9*, *Fnbp1l*, *Gdi1*, *Iqgap1*, *Itsn1*, *Pafah1b1*, *Pafah1b2/3*, *Pak3*, *Par6b*, *Rala*, and *Tnk2*. We microinjected the lentivirus particles into the seminiferous tubules of WT mice at 4 weeks after birth and examined the impact of shRNA by histological analysis. This method allows gene transduction into Sertoli cells because *in vivo* lentivirus transduction does not transduce germ cells (Ikawa et al., 2002). Of the tested samples, *Pafah1b* depletion showed a significant impact on testicular weight (Figure 2A). Histological analyses confirmed that *Pafah1b* depletion significantly impairs spermatogenesis (Figures 2B and 2C). Almost no germ cells were present in some of the seminiferous tubules.

To confirm that *Pafah1b1* depletion influences CDC42 activity, we used fluorescence resonance energy transfer (FRET) analysis. We produced adenoassociated viruses (AAVs) that express a FRET biosensor, AAV8-RaichuEV-Cdc42 (Komatsu et al., 2011). We used AAV8 capsid to specifically infect Sertoli cells (Watanabe et al., 2018). Therefore, the probe reflects the spatiotemporal activity of CDC42 in Sertoli cells *in vivo* (Figures S2A–S2G). Quantification of acquired images revealed that *Pafah1b1* depletion significantly reduces FRET/ECFP ratio in Sertoli cells (Figure 2D). These results suggested that PAFAH1B1 activates CDC42 in Sertoli cells.

Functional analyses of Cdc42-deficient testes using spermatogonial transplantation

To determine the impact of *Cdc42* deficiency on germ cells, we performed immunohistochemical staining using several germ cell markers (Figure 3A). We did not find significant differences in the number of undifferentiated spermatogonia that were positive for GFRA1 (a marker of A_{single}, A_{paired}, and some $A_{aligned}$ spermatogonia) or CDH1 (a marker for total undifferentiated spermatogonia) in 2-week-old testes. However, these testes already contained peanut agglutinin (PNA)-reactive haploid cells despite decreased expression of SYCP1 (zygotene to diplotene stage marker). Although SYCP3 (leptotene to diplotene stage marker) also showed decreased expression, the difference between KO and WT testes were not significant. No changes were found for γH2AX (intermediate spermatogonia to pachytene stage marker)

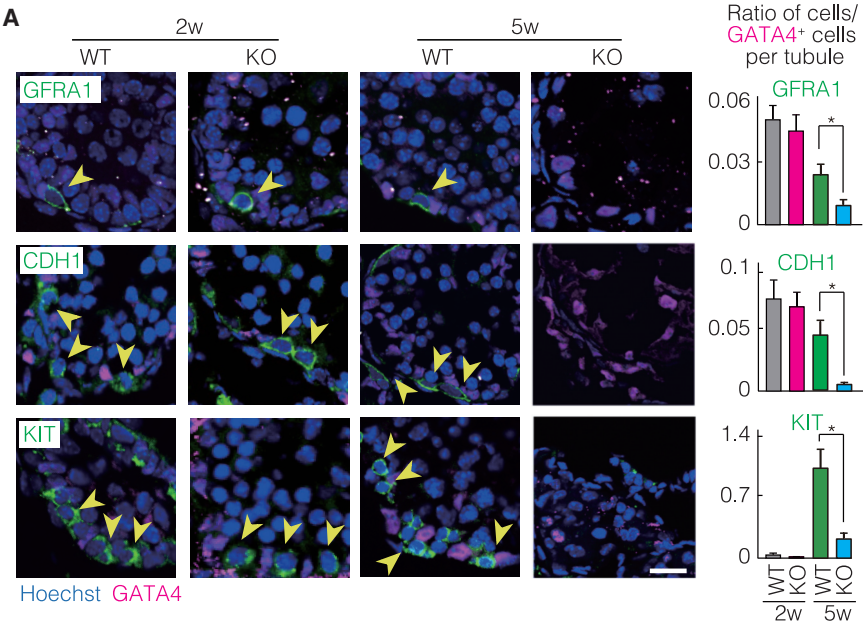

Figure 3. Functional analysis of SSCs and the microenvironment in Sertoli-specific *Cdc42*-deficient mice

(A) Immunostaining of *Cdc42*-deficient testes with Sertoli (GATA4) and germ cell markers. At least 42 tubules were counted for each marker. Arrowheads indicate cells with germ cell markers.

(B) Macroscopic appearance of WT recipient testis transplanted with *Cdc42*-deficient donor mouse testis cells.

(C) Colony counts (n = 16).

(D) Lectin (PNA) immunostaining of WT recipient testes transplanted with *Cdc42*-deficient donor mouse testis cells.

(E) Macroscopic appearance of *Cdc42*-deficient recipient testis transplanted with WT donor mouse testis cells.

(F) Colony counts (n = 8).

(G) Lectin (PNA) immunostaining of *Cdc42*-deficient recipient testes transplanted with WT donor mouse testis cells.

Bar, 20 μm (A, D, and G), 1 mm (B and E). Stain, Hoechst 33342 (A, D, and G). Asterisk indicates statistical significance ($p < 0.05$). See also Figure S3.

(Figure S3). However, the difference in the number of cells expressing meiotic markers became more pronounced by 3 weeks, and all of the examined meiotic markers were significantly decreased. Very few meiotic cells were found in 5-week old KO testes. These results suggested that abnormal meiosis produced PNA$^+$ haploid cells prematurely in *Cdc42* KO mice.

Concomitant with the loss of meiotic cells, spermatogonia number also gradually decreased during postnatal development. Although no significant changes were found in the number or pattern of spermatogonia cell populations 2 weeks after birth, we noted lower numbers of GFRA1$^+$ or CDH1$^+$ undifferentiated spermatogonia in the testes of 5-week-old *Cdc42*-deficient mice (Figure 3A). Accordingly, there was a decrease in the number of KIT$^+$ differentiating spermatogonia. This result suggests that CDC42 expression in Sertoli cells is necessary for maintaining primitive germ cell populations, which may include SSCs.

To confirm the effects of Sertoli cell-specific *Cdc42* deficiency on SSCs, we performed spermatogonial transplantation (Brinster and Zimmermann, 1994). To introduce a fluorescent donor cell marker, we used C57BL6/Tg14(act-EGFP-OsbY01) (green) mice to produce *Cdc42*-deficient mice expressing the *Egfp* transgene. Testes from 8-week-old *Cdc42*-deficient donor mice were transplanted into the seminiferous tubules of WT mice treated with busulfan, which depletes endogenous germ cells. Two months after transplantation, recipient mice showed a significant loss of SSCs (Figure 3B). *Cdc42*-deficient and WT control cells generated 0.1 and 8.3 colonies per 10^5 transplanted cells, respectively (Figure 3C). Lectin immunostaining of recipient testes confirmed haploid cell formation from WT donor cells (Figure 3D). Because Sertoli cell-specific *Cdc42* deficiency significantly reduced germ cell development, we reasoned that SSCs could have been enriched in *Cdc42*-deficient testes if SSCs remained are functionally normal and retain the ability of recolonizing the seminiferous tubules. However, significantly reduced colonization of *Cdc42*-deficient donor testes suggested that *Cdc42* in Sertoli cells is required for SSC development.

We also performed reciprocal transplantation experiments to test whether *Cdc42*-deficient Sertoli cells allow for colonization of WT SSCs. *Cdc42*-deficient and WT mice were treated with busulfan to eliminate endogenous spermatogenesis. After 35 days, when recipient germ cells were eliminated, we microinjected testis cells from WT green mice. The recipient *Cdc42*-deficient mice showed reduced donor cell colonization (Figure 3E). Testes from WT recipients contained 18.4 colonies per 10^5 cells,

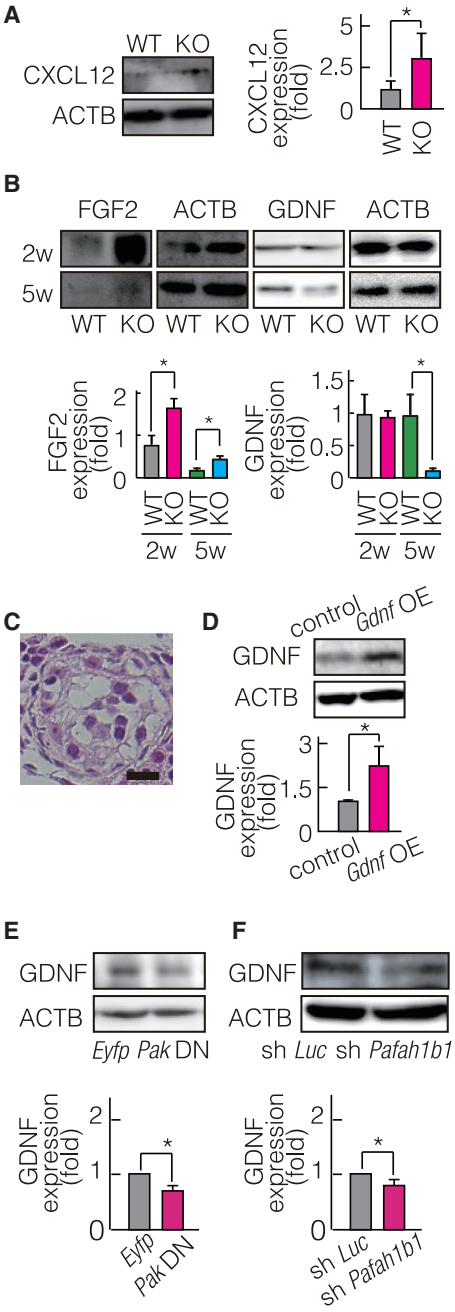

Figure 4. Reduced GDNF expression in Sertoli-specific *Cdc42*-deficient testes

(A) Western blot analysis of CXCL12 in 5-week-old *Cdc42*-deficient testes (n = 3).

(B) Western blot analysis of GDNF and FGF2 in 2- and 5-week-old *Cdc42*-deficient testes (n = 6).

(C) Histological analysis of *Cdc42*-deficient testis microinjected with a *Gdnf*-expressing lentivirus.

(D) Western blot analysis of GDNF in 5- to 10-day-old *Cdc42*-deficient testes microinjected with a *Gdnf*-expressing lentivirus 1 week after microinjection (n = 6).

(E and F) Western blot analysis of GDNF in 4-week-old *Cdc42*-deficient testes microinjected with lentiviruses expressing *Pak1* DN (E) or *Pafah1b1* shRNA (F) 1 week after microinjection (n = 10). Asterisk indicates statistical significance ($p < 0.05$). Bar, 20 μm (C). Stain, hematoxylin and eosin (C).

while very few colonies were generated in *Cdc42*-deficient testes (Figure 3F). Lectin immunostaining of WT recipient testes showed normal haploid cell formation (Figure 3G). These results suggested that *Cdc42*-deficient mice failed to accommodate donor-derived spermatogenesis.

Reduced GDNF expression in Cdc42-deficient testes

Since the results of the transplantation experiments suggested a significant loss of SSCs in testes of *Cdc42*-deficient mice, we hypothesized that SSC deficiency might be caused by impaired niche function. This is because SSCs from WT testes failed to colonize the seminiferous tubules of *Cdc42*-deficient mice, which suggested that *Cdc42*-deficient Sertoli cells may lack chemotactic factors for migrating to the niche. Alternatively, a deficiency in self-renewal factors may compromise SSC survival or expansion. To distinguish between these two possibilities, we used western blot analyses to measure CXCL12 expression in the testes of adult *Cdc42*-deficient mice. CXCL12 is a chemokine that attracts SSCs to the germline niche (Kanatsu-Shinohara et al., 2012; Yang et al., 2013). CXCL12 expression levels were higher in the testes of *Cdc42*-deficient mice (Figure 4A), which suggested that other niche-derived signals may be affecting SSC migration.

FGF2 and GDNF are major drivers of SSC self-renewal (Ishii et al., 2012; Meng et al., 2000). Therefore, we examined their expression at 2 and 5 weeks after birth because abnormal spermatogenesis was not evident at 2 weeks. Western blot analysis showed that testes of 2-week-old *Cdc42*-deficient mice had higher FGF2 expression than WT mice (Figure 4B). Although its expression decreased in 5-week-old testes, *Cdc42* KO testes still expressed FGF2 more strongly than WT testes. GDNF expression levels in the testes of 2-week-old *Cdc42*-deficient mice were comparable to those of WT mice, although, at 5 weeks, *Cdc42* KO testes showed reduced GDNF expression. These results suggested that impaired spermatogenesis was associated with abnormal GDNF expression. However, when we tried to rescue defective spermatogenesis by transfection of *Gdnf* in immature *Cdc42*-deficient pup testes, we were unable to see restoration of spermatogenesis (Figure 4C), despite significant increase in GDNF expression levels (Figure 4D). This suggested that additional factors are involved in this defect.

Because CDC42 can directly bind to the kinase PAK1, we examined whether inhibition of PAK1 might influence GDNF expression. We microinjected lentivirus particles expressing *Pak1* dominant-negative (DN) cDNA and examined GDNF expression. Western blot analysis showed significant downregulation of GDNF (Figure 4E). We also confirmed that GDNF expression is downregulated after *Pafah1b1* depletion (Figure 4F). Taken together, these results suggested that aberrant regulation of CDC42 activity is also associated with GDNF downregulation via PAK1.

Reduced localization of phosphorylated MAPK1/3 in the nucleus of Cdc42-deficient Sertoli cells

Because *Gdnf* is regulated by the MAP2K1 pathway (Hasegawa et al., 2013), we analyzed *Gdnf* expression using real-time polymerase chain reaction (PCR). We microinjected the MAP2K1 inhibitor PD0325901 (PD) into the seminiferous tubules of WT

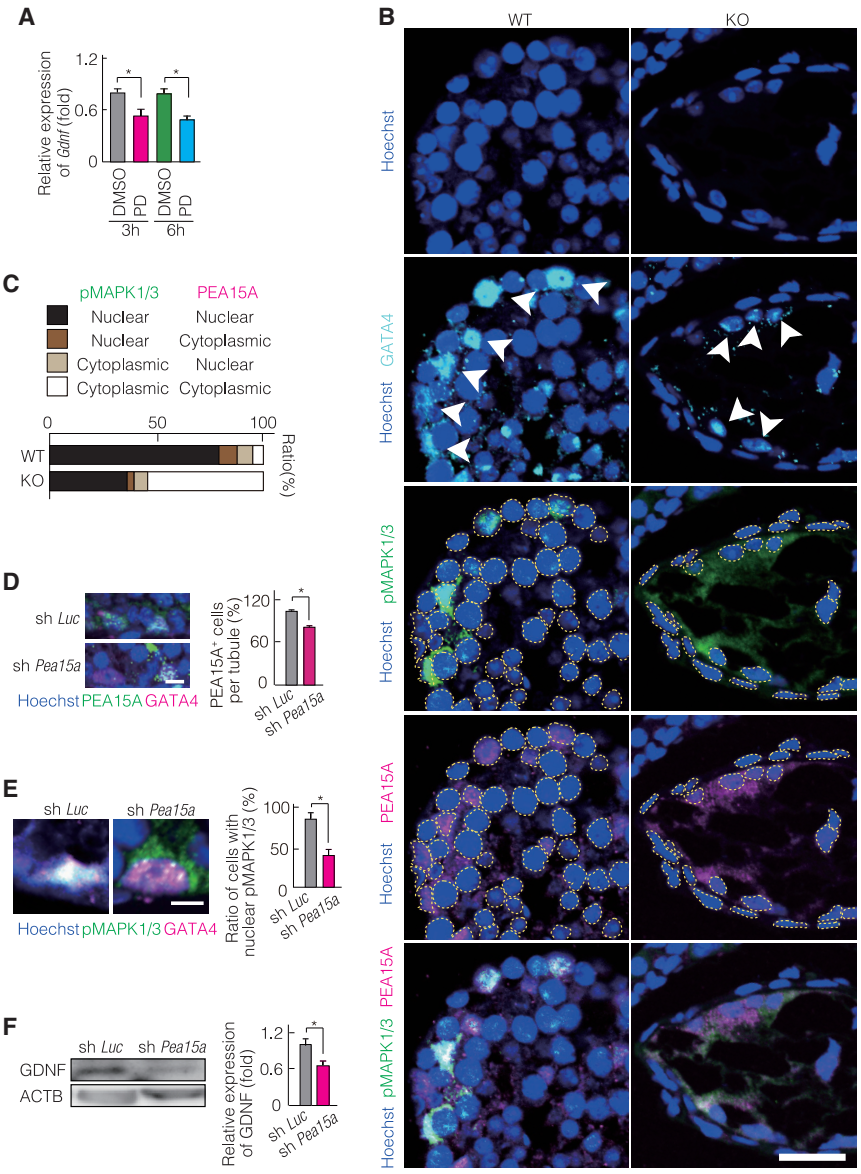

Figure 5. Regulation of GDNF expression by the MAP2K1 pathway

(A) Real-time PCR analysis of *Gdnf* expression after microinjection of PD into WT testes (n = 3).

(B and C) Immunostaining (B) and quantification (C) of Sertoli cells in *Cdc42*-deficient testes with GATA4, phosphorylated MAPK1/3 (pMAPK1/3), and PEA15A antibodies. Nuclear outlines are indicated by broken lines. GATA4 expression in Sertoli cells are indicated by arrowheads. At least 12 tubules were counted.

(D) Immunostaining of WT testes with pMAPK1/3 and PEA15A antibodies after microinjection of shRNA against *Pea15a*. At least eight tubules were counted.

(E) Immunostaining of WT testes with PEA15A antibody after microinjection of *Pea15* shRNA. At least 12 tubules were counted.

(F) Western blot analysis of WT testes that received *Pea15a* shRNA (n = 4). Testes were recovered 1 week after microinjection.

Bar, 5 μm (B and E) and 10 μm (D). Stain, Hoechst 33342 (B, D, and E). Asterisk indicates statistical significance ($p < 0.05$).

mouse testes. Testes treated with PD showed significant downregulation of *Gdnf* as early as 3 h after microinjection (Figure 5A). To understand how the MAP2K1 pathway regulates *Gdnf*, we performed immunostaining for phosphorylated MAPK1/3 (pMAPK1/3) (Figure 5B). In the testes of WT mice, pMAPK1/3 was found predominantly in the nucleus of Sertoli cells. However, in *Cdc42*-deficient mice, pMAPK1/3 was found mostly in the cytoplasm.

We next focused on PEA15A, a scaffolding protein known to regulate MAPK1/3 location (Fiory et al., 2009). We analyzed PEA15A expression because *Pea15a* KO mice show abnormal spermatogenesis (Mizrak et al., 2007). WT Sertoli cells expressed PEA15A mostly in the nucleus, while *Cdc42*-deficientt Sertoli cells expressed PEA15A in the nucleus and in the cytoplasm (Figures 5B and 5C). Since the distribution of PEA15A resembled pMAPK1/3, PEA15A may be one of the MAPK1/3 scaffold proteins to retain MAPK1/3 in the nucleus. However, because PEA15A promotes or inhibits MAPK1/3 signaling dependent on the cell type (Sulzmaier et al., 2012), we depleted *Pea15a* expression. We found that microinjection of lentiviruses expressing shRNA against *Pea15a* into the seminiferous tubules of WT mice reduced the number of PEA15A$^+$ Sertoli cells to ~70% (Figure 5D) and decreased the nuclear expression of pMAPK1/3 in Sertoli cells (Figure 5E).

Next, we used western blot analysis to examine the impact of reduced pMAPK1/3 in Sertoli cell nucleus and found that *Pea15a* depletion significantly reduced GDNF expression (Figure 5F). Because lentivirus injected into the seminiferous tubules cannot infect germ cells (Ikawa et al., 2002), these results suggested that nuclear localization of pMAPK1/3 was associated with GDNF expression and that there was a significant reduction of nuclear pMAPK1/3 in *Cdc42*-deficient mice, which downregulated GDNF expression.

Downregulation of DMRT1 and SOX8/9 in Cdc42-deficient Sertoli cells

We examined the expression of transcription factors that might be involved in GDNF expression. Previous studies revealed several candidate transcription factors that influence GDNF expression. We used western blotting to analyze whether these genes were expressed normally in *Cdc42*-deficient mice testes. Loss of DMRT1 or SOX8/SOX9 was reported to downregulate

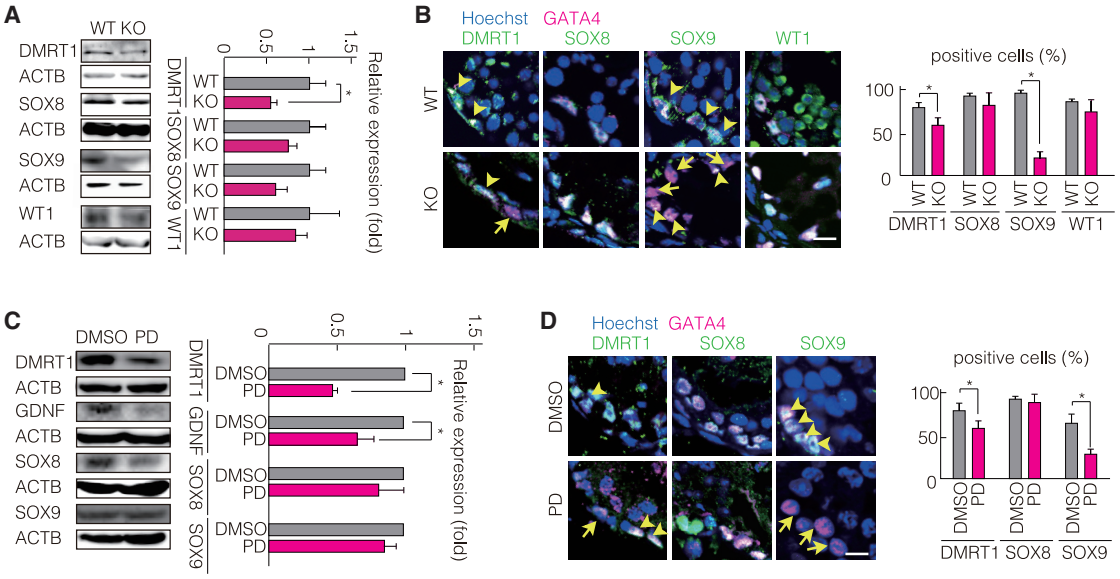

Figure 6. Downregulation of DMRT1 and SOX8/9 in *Cdc42*-deficient testis

(A) Western blot analysis of DMRT1 (n = 6), SOX8/9 (n = 5), and WT1 (n = 5) in busulfan-treated testes from *Cdc42*-deficient mice.

(B) Immunostaining of *Cdc42*-deficient testes with GATA4 and DMRT1, SOX8/9, or WT1 antibodies. At least 12 tubules were counted. Arrows indicate Sertoli cells lacking candidate proteins. Arrowheads indicate GATA4^{+} Sertoli cells with candidate protein expression.

(C) Western blot analysis of GDNF and candidate proteins following *in vitro* PD treatment (n = 7).

(D) Immunostaining of DMRT1 and SOX8/9 in WT testes following *in vitro* PD treatment. At least 12 tubules were counted. Arrows indicate Sertoli cells lacking candidate proteins. Arrowheads indicate GATA4^{+} Sertoli cells with candidate protein expression. Bar, 20 μm (B and D). Stain, Hoechst 33342 (B and D). Asterisk indicates statistical significance ($p < 0.05$).

GDNF (Barrionuevo et al., 2016; Chalmel et al., 2013; Krentz et al., 2013). We also analyzed WT1, because it is involved in the de-differentiation of Sertoli cells into Leydig cells (Zhang et al., 2015). To compare their expression levels in somatic cells, we removed germ cells using busulfan treatment because some of these genes are also expressed in germ cells. Western blot analysis showed significant downregulation of DMRT1 in *Cdc42*-deficient mice testes (Figure 6A). SOX8/9 and WT1 levels were also lower, although these differences were not significant.

To assess the protein distribution, we performed double immunostaining using antibodies against the Sertoli cell marker GATA4. Although apparent changes in SOX8 expression levels were not detectable, a significant proportion of Sertoli cells lacked SOX9 in *Cdc42*-deficient mice (Figure 6B). DMRT1 was also downregulated, albeit to a lesser degree. These results suggested that downregulation of critical Sertoli cell transcription factors contributed to reduced expression of GDNF in *Cdc42*-deficient mice.

We next examined whether DMRT1 and SOX9 are regulated by the MAP2K1 pathway. We used an organ culture system (Sato et al., 2011a) because microinjection of PD into the seminiferous tubules may not be effective due to diffusion. Testes from adult WT mice were severed into fragments and cultured on agarose gels. We added PD to the culture medium to inhibit MAP2K1. Western blot analysis confirmed significant downregulation of GDNF and DMRT1 in PD-treated cultures (Figure 6C). Although SOX8/SOX9 levels were downregulated, these differences were not significant. To examine protein distribution in Sertoli cells, we performed immunohistochemistry. Quantification of GATA4-expressing Sertoli cells showed that PD treatment reduced the proportion of cells expressing DMRT1 and SOX9 (Figure 6D). These results suggested that downregulation of DMRT1 and SOX9 decreased GDNF expression through MAP2K1 inhibition.

DISCUSSION

GDNF is a niche-derived signal that sustains SSCs *in vivo* (Meng et al., 2000). Regulation of GDNF expression appears to be complex. In one study, GDNF expression was increased upon treatment with FSH (Tadokoro et al., 2002), suggesting that it is positively regulated in Sertoli cells by the pituitary-gonadal axis. However, immunochemical studies revealed that GDNF is not expressed consistently in Sertoli cells; GDNF levels are high in stages V-VII of the seminiferous epithelial cycle but low in stages VIII-I (Sato et al., 2011b; Sharma and Braun, 2018). This heterogeneous expression pattern appears to reflect MAP2K1 activity since the inhibition of MAP2K1 suppressed GDNF expression (Hasegawa et al., 2013). This was also confirmed in our study. More recent studies also suggest that germ cells activate NOTCH signaling in Sertoli cells and downregulate GDNF (Garcia et al., 2014). Thus, GDNF relies on extragonadal signals as well as signals from germ cells.

Since GDNF is an SSC self-renewal factor, it is likely that SSC deficiency was caused by reduced GDNF expression in Sertoli cells. Indeed, loss of GDNF in *Gdnf* heterozygous KO mice results in gradual loss of spermatogenesis (Meng et al., 2000). Although the expression of GDNF was initially thought to be

limited to Sertoli cells, recent studies suggested that GDNF is also expressed in peritubular cells that surround the seminiferous tubules (Chen et al., 2016). In that experiment, conditional deletion of *Ar* in peritubular myoid cells decreased GDNF expression. Although *Ar*-deficient mice were initially fertile, they gradually became infertile due to decreased spermatogenesis and loss of undifferentiated spermatogonia, which suggests that peritubular cells also contribute to niche function. Moreover, most experiments that claim loss of SSCs depend on the morphological analysis of spermatogenesis; it is difficult to exclude the possibility of persistence of low numbers of SSCs. To confirm the loss of SSCs, we carried out spermatogonial transplantation experiments and showed that 8-weeek-old mice with *Cdc42*-deficient Sertoli cells had low numbers of SSCs. This result not only indicated that Sertoli cell-specific CDC42 is responsible for SSC development but also suggested that GDNF produced by peritubular cells is not sufficient to support survival of SSCs. Further studies are required to investigate the role of GDNF derived from peritubular cells.

Because a lack of SSCs in *Cdc42*-deficient testes suggested that germ cells themselves became defective, we examined whether *Cdc42*-deficient Sertoli cells have appropriate microenvironment for SSCs. To confirm this point, we performed spermatogonial transplantation and transplanted mature SSCs from WT testes into *Cdc42*-deficient testes. As expected, transplantation experiments showed poor colonization in the testes of *Cdc42*-deficient mice, suggesting that the germline niche is not functionally established in the absence of *Cdc42*. CXCL12 and GDNF are prime candidates for SSC homing factors. Without CXCR4, a receptor for CXCL12, SSCs exhibited impaired homing activity (Kanatsu-Shinohara et al., 2012). However, given the relatively high expression of CXCL12 in *Cdc42*-deficient testes, it is likely that reduced GDNF expression decreased homing of transplanted SSCs. Moreover, because GDNF increases the CXCR4 levels in cultured SSCs (Kanatsu-Shinohara et al., 2012), reduced expression of GDNF in *Cdc42*-deficient mice may exacerbate homing defects despite relatively high expression levels of CXCL12. In addition, reduction of GDNF in *Cdc42*-deficient testes might not be sufficient to support the survival of SSCs that have successfully migrated.

Our study suggests that *Cdc42* regulates transcription factors in the testes via the MAP2K1-MAPK1/3 signaling pathway. MAP2K1 activation regulates GDNF (Hasegawa et al., 2013), though the mechanisms are unclear. There was a significant reduction of pMAPK1/3 in the nuclei of *Cdc42*-deficient Sertoli cells. CDC42 can influence several signaling pathways, including the MAP2K1 pathway (Zhong et al., 2003). PEA15A is one of the scaffold proteins that regulate MAPK1/3 location (Fiory et al., 2009), and the amount of nuclear PEA15A was significantly decreased in *Cdc42*-deficient Sertoli cells. In addition, *Pea15a* KO mice showed increased apoptosis in spermatogonia (Mizrak et al., 2007). Although it was not clear whether PEA15A in germ or Sertoli cells is important, we hypothesized that PEA15A contributes to the nuclear retention of pMAPK1/3. As expected, when *Pea15a* levels were decreased through shRNA, GDNF expression levels decreased in the testes of WT mice. Therefore, nuclear translocation and retention of pMAPK1/3 in the nucleus is a critical step in GDNF expression. However, compared with *Pea15a* KO mice (Mizrak et al., 2007), defects in spermatogenesis were more pronounced in *Cdc42*-deficient mice. Given the results of our *Pea15a* knockdown (KD) experiments, we speculate that *Cdc42* deficiency may disturb the localization of other scaffold proteins and cause abnormalities in MAP2K1-MAPK1/3 signaling in the testes.

By screening transcription factors, we found that DMRT1 and SOX9 are downregulated in the testes of *Cdc42*-deficient mice. However, western blot analysis of testes lysate did not reveal a significant downregulation of SOX8/9 in the testes of *Cdc42*-deficient mice. SOX8 levels did not change significantly with the loss of *Cdc42*, which may be a compensatory mechanism for SOX9 deficiency. Since DMRT1 and SOX9 contribute to sexual differentiation (Foster et al., 1994; Matson et al., 2011), their simultaneous downregulation may decrease GDNF expression. Indeed, *Dmrt1* mutants show ~2-fold downregulation of GDNF 15.5 dpc (Krentz et al., 2013). Likewise, prenatal *Sox9* deficiency by Amh-*Cre* transgenic mice induces a gradual loss of ZBTB16^{+} spermatogonia and double deletion of *Sox8*/*Sox9* depleted GDNF expression (Barrionuevo et al., 2016; Chalmel et al., 2013). We showed through our organ culture experiments that DMRT1 and SOX9 are regulated by the MAP2K1 pathway. The association between FGF signaling and SOX9 is suggested by several studies. For example, SOX9 and FGF9 form a positive feed-forward loop that increases and maintains their levels of expression during gonad development (Kim et al., 2006). Moreover, MAPK1/3 induces the expression of SOX9 and interacts with SOX9 in other cell types (Huang et al., 2000; Ling et al., 2011). Other studies show that both SOX8/SOX9 are necessary for maintaining *Dmrt1* expression during development and in the adult testes (Barrionuevo et al., 2009, 2016). Therefore, it is possible that deregulation of SOX9 expression leads to DMRT1 downregulation.

At least two questions arise from our present study. First is the mechanism of CDC42 regulation. We found that *Pafah1b1* depletion significantly impairs CDC42 activity and reduces GDNF expression. The link between *Pafah1b1* and CDC42 was previously described in neuronal motility (Kholmanskikh et al., 2006). For spermatogenesis, mice lacking testis specific *Pafah1b1* transcript exhibited abnormal spermatogenesis (Nayernia et al., 2003). However, this line still contains a residual *Pafah1b1* transcript and the function of *Pafah1b1* in Sertoli cells remains unknown. Because their testes still maintained spermatogonia, it is likely that GDNF is expressed in their testes. Future studies are required to determine the function of *Pafah1b1* in Sertoli cells by completely removing this gene by gene targeting.

The second question is regarding the possible existence of other additional self-renewal factors. While our results strongly suggest that GDNF deficiency causes spermatogenic defects in *Cdc42*-deficient mice, we speculate that other self-renewal signals are compromised in these mice. This is because some SSCs can survive in the absence of GDNF *in vitro* and supplementation with FGF2 promoted the proliferation (Takashima et al., 2015). In that study, we also analyzed *Ret*^{Y1062F} mutant testes. RET is a component of GDNF receptor and *Ret* mutant testes also exhibited gradual loss of spermatogenesis. However, these testes still contained a small number of proliferating

undifferentiated spermatogonia. Because these cells were found in mature animals, they likely included SSCs. Therefore, *Gdnf* deficiency alone may not deplete SSCs. Because FGF2 levels were increased in the testes of *Cdc42*-deficient mice, the GDNF-independent SSC population likely persisted even in the absence of *Cdc42*. Given the significant loss of SSCs in this study, it is possible that testes from *Cdc42*-deficient mice also lack additional self-renewal signals.

Characterization of the germline niche is an important step for understanding the regulation of SSCs. This study used spermatogonial transplantation technique to show that CDC42 in Sertoli cells is required for development of the germline niche. This result contrasts with a recent study on *Rac1* in Sertoli cells, which did not show abnormalities in niche function but showed defective BTB (Heinrich et al., 2020). Future studies should seek to understand how *Cdc42* is regulated and identify additional regulators of niche development. Such analyses will be useful not only for understanding germ cell development but also for treating male infertility.

STAR★METHODS

Detailed methods are provided in the online version of this paper and include the following:

- KEY RESOURCES TABLE
- RESOURCE AVAILABILITY
  - Lead contact
  - Materials availability
  - Data and code availability
- EXPERIMENTAL MODEL AND SUBJECT DETAILS
  - Mice
- METHOD DETAILS
  - Virus preparation
  - Microinjection
  - *In vivo* imaging of testes with FRET biosensor and its image processing
  - Real-time PCR
- QUANTIFICATION AND STATISTICAL ANALYSIS

SUPPLEMENTAL INFORMATION

Supplemental information can be found online at https://doi.org/10.1016/j.celrep.2021.109550.

ACKNOWLEDGMENTS

We thank Ms. S. Ikeda for technical assistance. Financial support for this research was provided by AMED (17933225 and JP19gm1110008) and MEXT (19K22512, 19H05750, 19H04906, 18H04882, 18H05281, and 18H02935). This work was supported by Kyoto University Live Imaging Center.

AUTHOR CONTRIBUTIONS

Y.M. carried out most of the experiments. S.T. and M.K.-S. maintained and analyzed mutants. T.S. performed spermatogonial transplantation. Y.M. and T.S. designed the experiments. Y.M., M.K.-S., and T.S. and wrote the manuscript.

DECLARATION OF INTERESTS

The authors declare no competing interests.

Received: May 4, 2020
Revised: May 31, 2021
Accepted: July 27, 2021
Published: August 17, 2021.

REFERENCES

Barrionuevo, F., Georg, I., Scherthan, H., Lécureuil, C., Guillou, F., Wegner, M., and Scherer, G. (2009). Testis cord differentiation after the sex determination stage is independent of Sox9 but fails in the combined absence of Sox9 and Sox8. Dev. Biol. *327*, 301–312.

Barrionuevo, F.J., Hurtado, A., Kim, G.-J., Real, F.M., Bakkali, M., Kopp, J.L., Sander, M., Scherer, G., Burgos, M., and Jiménez, R. (2016). Sox9 and Sox8 protect the adult testis from male-to-female genetic reprogramming and complete degeneration. eLife *5*, e15635.

Brinster, R.L., and Zimmermann, J.W. (1994). Spermatogenesis following male germ-cell transplantation. Proc. Natl. Acad. Sci. USA *91*, 11298–11302.

Chalmel, F., Lardenois, A., Georg, I., Barrionuevo, F., Demougin, P., Jégou, B., Scherer, G., and Primig, M. (2013). Genome-wide identification of Sox8-, and Sox9-dependent genes during early post-natal testis development in the mouse. Andrology *1*, 281–292.

Chen, L.Y., Willis, W.D., and Eddy, E.M. (2016). Targeting the Gdnf Gene in peritubular myoid cells disrupts undifferentiated spermatogonial cell development. Proc. Natl. Acad. Sci. USA *113*, 1829–1834.

De Gendt, K., Denolet, E., Willems, A., Daniels, V.W., Clinckemalie, L., Denayer, S., Wilkinson, M.F., Claessens, F., Swinnen, J.V., and Verhoeven, G. (2011). Expression of Tubb3, a beta-tubulin isotype, is regulated by androgens in mouse and rat Sertoli cells. Biol. Reprod. *85*, 934–945.

de Rooij, D.G., and Russell, L.D. (2000). All you wanted to know about spermatogonia but were afraid to ask. J. Androl. *21*, 776–798.

Erickson, J.W., and Cerione, R.A. (2001). Multiple roles for Cdc42 in cell regulation. Curr. Opin. Cell Biol. *13*, 153–157.

Etienne-Manneville, S. (2004). Cdc42–the centre of polarity. J. Cell Sci. *117*, 1291–1300.

Fiory, F., Formisano, P., Perruolo, G., and Beguinot, F. (2009). Frontiers: PED/PEA-15, a multifunctional protein controlling cell survival and glucose metabolism. Am. J. Physiol. Endocrinol. Metab. *297*, E592–E601.

Foster, J.W., Dominguez-Steglich, M.A., Guioli, S., Kwok, C., Weller, P.A., Stevanović, M., Weissenbach, J., Mansour, S., Young, I.D., Goodfellow, P.N., et al. (1994). Campomelic dysplasia and autosomal sex reversal caused by mutations in an SRY-related gene. Nature *372*, 525–530.

França, L.R., Hess, R.A., Dufour, J.M., Hofmann, M.C., and Griswold, M.D. (2016). The Sertoli cell: one hundred fifty years of beauty and plasticity. Andrology *4*, 189–212.

Garcia, T.X., Farmaha, J.K., Kow, S., and Hofmann, M.C. (2014). RBPJ in mouse Sertoli cells is required for proper regulation of the testis stem cell niche. Development *141*, 4468–4478.

Gow, A., Southwood, C.M., Li, J.S., Pariali, M., Riordan, G.P., Brodie, S.E., Danias, J., Bronstein, J.M., Kachar, B., and Lazzarini, R.A. (1999). CNS myelin and sertoli cell tight junction strands are absent in Osp/claudin-11 null mice. Cell *99*, 649–659.

Hasegawa, K., Namekawa, S.H., and Saga, Y. (2013). MEK/ERK signaling directly and indirectly contributes to the cyclical self-renewal of spermatogonial stem cells. Stem Cells *31*, 2517–2527.

Heinrich, A., Potter, S.J., Guo, L., Ratner, N., and DeFalco, T. (2020). Distinct roles for Rac1 in Sertoli cell function during testicular development and spermatogenesis. Cell Rep. *31*, 107513.

Hiratsuka, T., Fujita, Y., Naoki, H., Aoki, K., Kamioka, Y., and Matsuda, M. (2015). Intercellular propagation of extracellular signal-regulated kinase activation revealed by in vivo imaging of mouse skin. eLife *4*, e05178.

Huang, W., Zhou, X., Lefebvre, V., and de Crombrugghe, B. (2000). Phosphorylation of SOX9 by cyclic AMP-dependent protein kinase A enhances SOX9's ability to transactivate a Col2a1 chondrocyte-specific enhancer. Mol. Cell. Biol. *20*, 4149–4158.

Ikawa, M., Tergaonkar, V., Ogura, A., Ogonuki, N., Inoue, K., and Verma, I.M. (2002). Restoration of spermatogenesis by lentiviral gene transfer: offspring from infertile mice. Proc. Natl. Acad. Sci. USA *99*, 7524–7529.

Ikawa, M., Yamada, S., Nakanishi, T., and Okabe, M. (1998). Green mice' and their potential usage in biological research. FEBS Lett *430*, 83–87.

Ishii, K., Kanatsu-Shinohara, M., Toyokuni, S., and Shinohara, T. (2012). FGF2 mediates mouse spermatogonial stem cell self-renewal via upregulation of Etv5 and Bcl6b through MAP2K1 activation. Development *139*, 1734–1743.

Kanatsu-Shinohara, M., Inoue, K., Takashima, S., Takehashi, M., Ogonuki, N., Morimoto, H., Nagasawa, T., Ogura, A., and Shinohara, T. (2012). Reconstitution of mouse spermatogonial stem cell niches in culture. Cell Stem Cell *11*, 567–578.

Kanatsu-Shinohara, M., Ogonuki, N., Matoba, S., Ogura, A., and Shinohara, T. (2020). Autologous transplantation of spermatogonial stem cells restores fertility in congenitally infertile mice. Proc. Natl. Acad. Sci. USA *117*, 7837–7844.

Kholmanskikh, S.S., Koeller, H.B., Wynshaw-Boris, A., Gomez, T., Letourneau, P.C., and Ross, M.E. (2006). Calcium-dependent interaction of Lis1 with IQGAP1 and Cdc42 promotes neuronal motility. Nat. Neurosci. *9*, 50–57.

Kim, Y., Kobayashi, A., Sekido, R., DiNapoli, L., Brennan, J., Chaboissier, M.-C., Poulat, F., Behringer, R.R., Lovell-Badge, R., and Capel, B. (2006). Fgf9 and Wnt4 act as antagonistic signals to regulate mammalian sex determination. PLoS Biol. *4*, e187.

Kitajiri, S., Miyamoto, T., Mineharu, A., Sonoda, N., Furuse, K., Hata, M., Sasaki, H., Mori, Y., Kubota, T., Ito, J., et al. (2004). Compartmentalization established by claudin-11-based tight junctions in stria vascularis is required for hearing through generation of endocochlear potential. J. Cell Sci. *117*, 5087–5096.

Komatsu, N., Aoki, K., Yamada, M., Yukinaga, H., Fujita, Y., Kamioka, Y., and Matsuda, M. (2011). Development of an optimized backbone of FRET biosensors for kinases and GTPases. Mol. Biol. Cell *22*, 4647–4656.

Krentz, A.D., Murphy, M.W., Zhang, T., Sarver, A.L., Jain, S., Griswold, M.D., Bardwell, V.J., and Zarkower, D. (2013). Interaction between DMRT1 function and genetic background modulates signaling and pluripotency to control tumor susceptibility in the fetal germ line. Dev. Biol. *377*, 67–78.

Lécureuil, C., Fontaine, I., Crepieux, P., and Guillou, F. (2002). Sertoli and granulosa cell-specific Cre recombinase activity in transgenic mice. Genesis *33*, 114–118.

Ling, S., Chang, X., Schultz, L., Lee, T.K., Chaux, A., Marchionni, L., Netto, G.J., Sidransky, D., and Berman, D.M. (2011). An EGFR-ERK-SOX9 signaling cascade links urothelial development and regeneration to cancer. Cancer Res. *71*, 3812–3821.

Lui, W.Y., Mruk, D.D., and Cheng, C.Y. (2005). Interactions among IQGAP1, Cdc42, and the cadherin/catenin protein complex regulate Sertoli-germ cell adherens junction dynamics in the testis. J. Cell. Physiol. *202*, 49–66.

Matson, C.K., Murphy, M.W., Sarver, A.L., Griswold, M.D., Bardwell, V.J., and Zarkower, D. (2011). DMRT1 prevents female reprogramming in the postnatal mammalian testis. Nature *476*, 101–104.

Meistrich, M.L., and van Beek, M.E.A.B. (1993). Spermatogonial stem cells. In Cell and molecular biology of the testis, C.C. Desjardins and L.L. Ewing, eds. (Oxford University Press), pp. 266–295.

Melendez, J., Liu, M., Sampson, L., Akunuru, S., Han, X., Vallance, J., Witte, D., Shroyer, N., and Zheng, Y. (2013). Cdc42 coordinates proliferation, polarity, migration, and differentiation of small intestinal epithelial cells in mice. Gastroenterology *145*, 808–819.

Meng, X., Lindahl, M., Hyvönen, M.E., Parvinen, M., de Rooij, D.G., Hess, M.W., Raatikainen-Ahokas, A., Sainio, K., Rauvala, H., Lakso, M., et al. (2000). Regulation of cell fate decision of undifferentiated spermatogonia by GDNF. Science *287*, 1489–1493.

Mizrak, S.C., Renault-Mihara, F., Párraga, M., Bogerd, J., van de Kant, H.J.G., López-Casas, P.P., Paz, M., del Mazo, J., and de Rooij, D.G. (2007). Phosphoprotein enriched in astrocytes-15 is expressed in mouse testis and protects spermatocytes from apoptosis. Reproduction *133*, 743–751.

Morimoto, H., Kanatsu-Shinohara, M., and Shinohara, T. (2015). ROS-generating oxidase Nox3 regulates the self-renewal of mouse spermatogonial stem cells. Biol. Reprod. *92*, 147.

Mruk, D.D., and Cheng, C.Y. (2015). The mammalian blood-testis barrier: its biology and regulation. Endocr. Rev. *36*, 564–591.

Nagano, M., Avarbock, M.R., and Brinster, R.L. (1999). Pattern and kinetics of mouse donor spermatogonial stem cell colonization in recipient testes. Biol. Reprod. *60*, 1429–1436.

Nayernia, K., Vauti, F., Meinhardt, A., Cadenas, C., Schweyer, S., Meyer, B.I., Schwandt, I., Chowdhury, K., Engel, W., and Arnold, H.H. (2003). Inactivation of a testis-specific Lis1 transcript in mice prevents spermatid differentiation and causes male infertility. J. Biol. Chem. *278*, 48377–48385.

Ogawa, T., Aréchaga, J.M., Avarbock, M.R., and Brinster, R.L. (1997). Transplantation of testis germinal cells into mouse seminiferous tubules. Int. J. Dev. Biol. *41*, 111–122.

Sarbassov, D.D., Guertin, D.A., Ali, S.M., and Sabatini, D.M. (2005). Phosphorylation and regulation of Akt/PKB by the rictor-mTOR complex. Science *307*, 1098–1101.

Sato, T., Katagiri, K., Gohbara, A., Inoue, K., Ogonuki, N., Ogura, A., Kubota, Y., and Ogawa, T. (2011a). In vitro production of functional sperm in cultured neonatal mouse testes. Nature *471*, 504–507.

Sato, T., Aiyama, Y., Ishii-Inagaki, M., Hara, K., Tsunekawa, N., Harikae, K., Uemura-Kamata, M., Shinomura, M., Zhu, X.B., Maeda, S., et al. (2011b). Cyclical and patch-like GDNF distribution along the basal surface of Sertoli cells in mouse and hamster testes. PLoS ONE *6*, e28367.

Sharma, M., and Braun, R.E. (2018). Cyclical expression of GDNF is required for spermatogonial stem cell homeostasis. Development *145*, dev151555.

Shinohara, T., Orwig, K.E., Avarbock, M.R., and Brinster, R.L. (2001). Remodeling of the postnatal mouse testis is accompanied by dramatic changes in stem cell number and niche accessibility. Proc. Natl. Acad. Sci. USA *98*, 6186–6191.

Stanton, P.G. (2016). Regulation of the blood-testis barrier. Semin. Cell Dev. Biol. *59*, 166–173.

Sulzmaier, F.J., Valmiki, M.K.G., Nelson, D.A., Caliva, M.J., Geerts, D., Matter, M.L., White, E.P., and Ramos, J.W. (2012). PEA-15 potentiates H-Ras-mediated epithelial cell transformation through phospholipase D. Oncogene *31*, 3547–3560.

Tadokoro, Y., Yomogida, K., Ohta, H., Tohda, A., and Nishimune, Y. (2002). Homeostatic regulation of germinal stem cell proliferation by the GDNF/FSH pathway. Mech. Dev. *113*, 29–39.

Takashima, S., Kanatsu-Shinohara, M., Tanaka, T., Morimoto, H., Inoue, K., Ogonuki, N., Jijiwa, M., Takahashi, M., Ogura, A., and Shinohara, T. (2015). Functional differences between GDNF-dependent and FGF2-dependent mouse spermatogonial stem cell self-renewal. Stem Cell Reports *4*, 489–502.

Ventura, A., Meissner, A., Dillon, C.P., McManus, M., Sharp, P.A., Van Parijs, L., Jaenisch, R., and Jacks, T. (2004). Cre-lox-regulated conditional RNA interference from transgenes. Proc. Natl. Acad. Sci. USA *101*, 10380–10385.

Watanabe, S., Kanatsu-Shinohara, M., Ogonuki, N., Matoba, S., Ogura, A., and Shinohara, T. (2017). Adeno-associated virus-mediated delivery of genes to mouse spermatogonial stem cells. Biol. Reprod. *96*, 221–231.

Watanabe, S., Kanatsu-Shinohara, M., Ogonuki, N., Matoba, S., Ogura, A., and Shinohara, T. (2018). In vivo genetic manipulation of spermatogonial stem cells and their microenvironment by adeno-associated viruses. Stem Cell Reports *10*, 1551–1564.

Wong, E.W., Mruk, D.D., Lee, W.M., and Cheng, C.Y. (2010). Regulation of blood-testis barrier dynamics by TGF-beta3 is a Cdc42-dependent protein trafficking event. Proc. Natl. Acad. Sci. USA *107*, 11399–11404.

Xiao, G.H., Beeser, A., Chernoff, J., and Testa, J.R. (2002). p21-activated kinase links Rac/Cdc42 signaling to merlin. J. Biol. Chem. *277*, 883–886.

Yang, L., Wang, L., Geiger, H., Cancelas, J.A., Mo, J., and Zheng, Y. (2007). Rho GTPase Cdc42 coordinates hematopoietic stem cell quiescence and niche interaction in the bone marrow. Proc. Natl. Acad. Sci. USA *104*, 5091–5096.

Yang, Q.E., Kim, D., Kaucher, A., Oatley, M.J., and Oatley, J.M. (2013). CXCL12-CXCR4 signaling is required for the maintenance of mouse spermatogonial stem cells. J. Cell Sci. *126*, 1009–1020.

Zhang, L., Chen, M., Wen, Q., Li, Y., Wang, Y., Wang, Y., Qin, Y., Cui, X., Yang, L., Huff, V., and Gao, F. (2015). Reprogramming of Sertoli cells to fetal-like Leydig cells by Wt1 ablation. Proc. Natl. Acad. Sci. USA *112*, 4003–4008.

Zhong, B., Jiang, K., Gilvary, D.L., Epling-Burnette, P.K., Ritchey, C., Liu, J., Jackson, R.J., Hong-Geller, E., and Wei, S. (2003). Human neutrophils utilize a Rac/Cdc42-dependent MAPK pathway to direct intracellular granule mobilization toward ingested microbial pathogens. Blood *101*, 3240–3248.

STAR★METHODS

KEY RESOURCES TABLE

Reagent or resource	Source	Identifier
Antibodies		
Rat anti-mouse CD117 (KIT)	eBioscience	Cat#14-1171; RRID:AB_467434; Lot E03982-1632
Rabbit anti-mouse CDC42	Abcam	Cat#64533; RRID:AB_1310067; Lot GR3200090-2
Rat anti-mouse CDH1	Gift from Dr. Masatoshi Takeichi, RIKEN CDB	RRID: CVCL_A6WX
Rabbit anti-mouse CLDN11	Gift from Dr. Sachiko Tsukita, Teikyo University	N/A
Rabbit anti-mouse non-phospho (active) CTNNB1 (Ser33/37/Thr41)	Cell Signaling Technology	Cat#8814 (clone: D13A1); Lot 3
Rabbit anti-mouse CXCL12	Torrey Pines Biolabs	Cat#201; RRID:AB_2335896; Lot 010718
Goat anti-mouse DMRT1	Santa Cruz	Cat#104885X; Lot J2610
Goat anti-mouse FGF2	Santa Cruz	Cat#1390; RRID:AB_631496; Lot F1113
Goat anti-mouse GATA4	Santa Cruz	Cat#1237; Lot K1611
Rabbit anti-mouse GATA4	Abcam	Cat#84593; RRID:AB_10670538; Lot GR275402-1
Rabbit anti-mouse GDNF	Santa Cruz	Cat#328; RRID:AB_631570; Lot F2713
Rabbit anti-GFP	Medical & Biological Laboratories	Cat#598; RRID:AB_591819; Lot 081
Goat anti-mouse GFRA1	R&D Systems	Cat#AF560; RRID:AB_2110307; Lot BQE0514081
Rabbit anti-human phospho-histone H2A.X (γH2AX)	Cell Signaling Technology	Cat#2577; RRID:AB_2118010; Lot 4
Rabbit anti-mouse LAMININ	Sigma	Cat#L9393; RRID:AB_477163; Lot 054K4780
Rat anti-Occludin	Gift from Dr. Sachiko Tsukita, Teikyo University	N/A
Mouse anti-mouse PAFAH1B1	Santa Cruz, Dallas, TX	Cat#374586 (clone: H-7); RRID:AB_11008596; Lot H0217
Mouse anti-mouse PEA15A	Santa Cruz, Dallas, TX	Cat#166678 (clone H-3); RRID:AB_2236964; Lot B1418
Rabbit anti-mouse phospho-p44/42 MAPK (Erk1/2) (Thr202/Tyr204)	Cell Signaling Technology	Cat#9101S; RRID:AB_331646; Lot 26
Rabbit anti-mouse SOX8	Thermo Fisher Scientific	Cat#PA1-28072; RRID:AB_2196251; Lot UE2770328F
Goat anti-mouse SOX9	Santa Cruz	Cat#17341; RRID:AB_661281; Lot F1311
Rabbit anti-mouse SOX9	Santa Cruz	Cat#20095; RRID:AB_661282; Lot I1897
Rabbit anti-mouse SYCP1	Abcam	Cat#15090; RRID:AB_371671; Lot GR3184119-1
Rabbit anti-mouse SYCP3	Thermo Fisher Scientific	Cat#PA1-16764; RRID:AB_568727; Lot WD3244703A
Mouse anti-mouse TUBB3	Sigma	Cat#T5076; RRID:AB_532291; Lot 047K4852
Rabbit anti-mouse Vimentin	Cell Signaling Technology	Cat#5741 (clone: D21H3); RRID:AB_10695459; Lot 1
Rabbit anti-mouse WT1	Santa Cruz	Cat#192; RRID:AB_632611; Lot K0811
Alexa Fluor 488-conjugated donkey anti-goat IgG	Thermo Fisher Scientific	Cat#A-11055; RRID:AB_2534102; Lot 2059218

(*Continued on next page*)

Continued

Reagent or resource	Source	Identifier
Alexa Fluor 488-conjugated donkey anti-mouse IgG	Thermo Fisher Scientific	Cat#A-31570; RRID:AB_2536180; Lot 1226927
Alexa Fluor 488-conjugated Goat anti-rat IgG	Thermo Fisher Scientific	Cat#A-11006; RRID:AB_141373; Lot 2048174
Alexa Fluor 555-conjugated donkey anti-rabbit IgG	Thermo Fisher Scientific	Cat#A-31572; RRID:AB_162543; Lot 1945911
Alexa Fluor 647-conjugated goat anti-rat IgG	Thermo Fisher Scientific	Cat#A-21247; RRID:AB_141778; Lot 1696458
Alexa Fluor 647-conjugated donkey anti-goat IgG	Thermo Fisher Scientific	Cat#A-21447; RRID:AB_141844; Lot 774898
FITC-conjugated streptavidin	Becton Dickinson and Company	Cat#554060; Lot M058982
HRP-conjugated chicken anti-goat IgG	Santa Cruz	Cat#2953; RRID:AB_639230; Lot 10805
HRP-conjugated goat anti-mouse IgG	Cell Signaling Technology	Cat#7076S, RRID:AB_330924; Lot 27
HRP-conjugated goat anti-rabbit IgG	Cell Signaling Technology	Cat#7074S, RRID:AB_2099233; Lot 29
Alexa Fluor 647-conjugated mouse anti-human GATA4	Santa Cruz	Cat#25310 (clone: G-4); RRID:AB_627667; Lot C2417
Rhodamine-conjugated Peanut Agglutinin (PNA)	Vector Laboratories	Cat#RL-1072; RRID:AB_2336642; Lot ZF1115
Rhodamine-Phalloidin	Thermo Fisher Scientific	Cat#R415; RRID:AB_2572408; Lot 1810954
Bacterial and virus strains		
pAAV-CAG	Watanabe et al., 2018	Penn Vector Core
pLKO.1	Sigma (transferred to Open Biosystems)	https://www.sigmaaldrich.com/deepweb/assets/sigmaaldrich/product/documents/157/923/shclndbul.pdf
pSicoR	Ventura et al., 2004	Addgene plasmid: 11579
Chemicals, peptides, and recombinant proteins		
PD0325901	Stemgent	Cat# 04-0006-base
Experimental models: Organisms/strains		
Mouse: B6;SJL-Plekha5$^{Tg(AMH-cre)1Flor}$/Orl	The European Mouse Mutant Archive	EM: 00022
Mouse: Cdc42$^{loxP/loxP}$; B6(129S6/SvEvTac)-Cdc42$^{tm1Yizh/J}$	Tha Jackson Laboratory	JAX: 027576
Mouse: C57BL/6-Tg(CAG-EGFP) C14-Y01-FM131Osb	(Ikawa et al., 1998)	RBRC00267
Mouse: Cldn11^{tm1Sts}	Kitajiri et al., 2004	RRID:MGI:3055494
Mouse: WBB6F1-Kit^{W}/Klt^{W-v}/J	Japan SLC, Shizuoka, Japan	JAX:100410
Oligonucleotides		
Gdnf forward: TCCAACTGGGGGTCTACGG	This paper	N/A
Gdnf reverse: GCCACGACATCCCATAACTTCAT	This paper	N/A
Hprt forward: GCTGGTGAAAAGGACCTCT	This paper	N/A
Hprt reverse: CACAGGACTAGAACACCTGC	This paper	N/A
Recombinant DNA		
pAAV8-CAG-RaichuEV-Cdc42	This paper	RaichuEV cDNA: Dr. Michiyuki Matsuda, Kyoto University
CSII-EF1a-Gdnf-IRES-Puro	This paper	Gdnf cDNA: Dr. Mari Dezawa, Tohoku University
CSII-EF1a-*Pak1* DN-IRES-Puro	Xiao et al., 2002	Pak1 DN cDNA: Addgene Plasmid: 12216

(*Continued on next page*)

Continued

Reagent or resource	Source	Identifier
pLKO.1-sh *Arhgap1*	Open Biosystems	TRCN0000097234, TRCN0000097235, TRCN0000097236, TRCN0000097237, TRCN0000097238
pSicoR-sh *Arhgap32* (TGCAAGCCATAGGCAATTA)	This paper	N/A
pLKO.1-sh *Cdc42ep5* (TGGAGCACTCTCGATCTCA)	This paper	N/A
pLKO.1-sh *Diaph2*	Open Biosystems	TRCN0000108775, TRCN0000108776, TRCN0000108777, TRCN0000108778
pLKO.1-sh *Dock9*	Open Biosystems	TRCN0000142217
pLKO.1-sh *Fnbp1l*	Open Biosystems	TRCN0000201274, TRCN0000201739, TRCN0000201845, TRCN0000202309
pLKO.1-sh *Gdi1*	Open Biosystems	TRCN0000089416
pLKO.1-sh *Iqgap1*	Open Biosystems	TRCN0000034334, TRCN0000034335, TRCN0000034336, TRCN0000034337, TRCN0000034338
pLKO.1-sh *Itsn1*	Open Biosystems	TRCN0000026163, TRCN0000026196, TRCN0000111568
pLKO.1-sh *Luc*	Sarbassov et al., 2005	Addgene plasmid: 1864
pLKO.1-sh *Pafah1b1*	Open Biosystems	TRCN0000183439, TRCN0000183516, TRCN0000183873
pLKO.1-sh *Pafah1b2/3*	Open Biosystems	TRCN0000054523, TRCN0000054524, TRCN0000054525, TRCN0000054526, TRCN0000054527, TRCN0000098231, TRCN0000098232, TRCN0000098233
pLKO.1-sh *Pak3*	Open Biosystems	TRCN0000025156, TRCN0000025158
pLKO.1-sh *Par6b*	Open Biosystems	TRCN0000054683, TRCN0000054685
pLKO.1-sh *Pea15a*	Open Biosystems	TRCN0000105786, TRCN0000105787, TRCN0000105788, TRCN0000105789
pLKO.1-sh *Rala*	Open Biosystems	TRCN0000077719, TRCN0000077720, TRCN0000077721, TRCN0000077722
pLKO.1-sh *Tnk2*	Open Biosystems	TRCN0000023750, TRCN0000023752, TRCN0000023753
Software and algorithms		
Metamorph	This paper	https://www.moleculardevices.com/products/cellular-imaging-systems/acquisition-and-analysis-software/metamorph-microscopy#gref

RESOURCE AVAILABILITY

Lead contact

Further information and requests for resources and reagents should be directed to and will be fulfilled by the lead contact, Takashi Shinohara (tshinoha@virus.kyoto-u.ac.jp).

Materials availability

Key resources including details of key reagents are available in the Key resources table. This study did not generate any new reagents.

Data and code availability

- Data reported in this paper will be shared by the lead contact upon request.
- This paper does not report custom code.
- Any additional information to reanalyze the data reported in this paper is available from the lead contact upon request.

EXPERIMENTAL MODEL AND SUBJECT DETAILS

Mice

All experiments utilizing animals were approved by The Institutional Animal Care and Use Committee of Kyoto University. All animals were maintained under conditions of *ad libitum* water and food with constant light-dark cycles. Generation of *Cdc42*$^{f/f}$ mice has been described previously (Yang et al., 2007). Sertoli cell-specific *Cdc42* KO mice were generated by crossing homozygous *Cdc42*$^{f/f}$ mice with Amh-*Cre* transgenic mice (Lécureuil et al., 2002), and their offspring were used for analysis. For screening of CDC42 regulators, we used 4-week-old C57BL/6 (B6) × DBA/2 F1 (BDF1) mice. For transplantation experiments, we crossed Sertoli cell-specific *Cdc42* KO mice with green mice (gifted by Dr. M. Okabe, Osaka University, Osaka, Japan). *Cldn11* KO mice were gifted by Dr. S. Tsukita (Teikyo University, Tokyo, Japan). W mice were purchased from Japan SLC (Shizuoka, Japan). Only male mice were used for analysis and transplantation experiments.

METHOD DETAILS

Virus preparation

For shRNA-mediated gene KD using lentivirus, shRNAs against candidate genes were purchased from Open Biosystems (Huntsville, AL). We also overexpressed *Gdnf* or *Pak1* DN cDNA that lacks autoinhibitory domain (aa83-149) using CSII-EF1a-IRES-Puro. A mixture of lentiviral particles was used for transfection; pLKO1-scramble shRNA was used as a control (Addgene; Cambridge, MA). Preparation of virus particles was previously described (Morimoto et al., 2015). Virus concentration was measured using a lentivirus PCR titer kit (Abm. Inc., New York, NY) according to the manufacturer's protocol.

For AAV experiments, we generated an AAV vector that expresses RaichuEV-Cdc42 (a gift from Dr. M. Matsuda, Kyoto University, Kyoto, Japan) (Komatsu et al., 2011; Watanabe et al., 2018). Virus particles was produced using pAAV8 capsid to specifically infect Sertoli cells (Watanabe et al., 2018). Production and titration of AAVs were carried out, as previously described (Watanabe et al., 2017).

Microinjection

For cell transplantation, we treated 4-week-old BDF1 mice or *Cdc42*-defieicnt mice with 44 mg/kg busulfan (Sigma, St. Louis, MO). At least 1 month following busulfan, the animals were anesthetized and used for transplantation. WT BDF1 mice without busulfan treatment were microinjection with 2 μM PD (Stemgent, San Diego, CA) or shRNA (5×10^7 IFU/ml). For rescue of *Cdc42*-deficient testes, we microinjected a *Gdnf*-expressing lentivirus into 5- to 10-day-old pups before germ cell depletion.

For microinjection, glass needles were inserted into the seminiferous tubules via the efferent duct (Ogawa et al., 1997). Each injection filled 75%–85% of the seminiferous tubules.

In vivo imaging of testes with FRET biosensor and its image processing

Live imaging was carried out as described previously with a slight modification (Hiratsuka et al., 2015). In brief, we co-injected particles of AAV8 expressing Raichu-*Cdc42* (1.6×10^{10}) and lentivirus expressing shRNA against *Luc* or *Pafah1b1* (3×10^5) into the seminiferous tubules of WT B6 mice. One week after microinjection, the animals were anesthetized by 1.5% isoflurane (FUJIFILM Wako Pure Chemical Corporation, Osaka, Japan). Testis samples were placed on a cover glass after removal of epididymis. Z stack images were acquired by a two-photon excitation FV1200MPE-IX83 inverted microscopy with Silicon immersion oil (Olympus, Tokyo, Japan). We used an IR-cut filter, RDM690, two dichroic mirrors, DM505, DM570 (all from Olympus), and three emission filters, FF01-425/30 (Semrock, Rochester, NY) for second harmonic generation (SHG) imaging. BA460-500 (Olympus) and BA520-560 (Olympus) were used for ECFP and for FRET(YPet) imaging, respectively. Orientation of basal or lateral/apical compartments of the seminiferous tubules was confirmed by SHG signals using Imaris software (Bitplane AG, Zurich, Switzerland), which represent the fibrous collagen structures of the basement membrane. The FRET ratio was calculated by dividing YPet intensity by ECFP intensity in one Sertoli cell with Metamorph software (Molecular Device, San Jose, CA).

Real-time PCR

Total RNA was isolated using TRIzol (Invitrogen, Carlsbad, CA). First-strand cDNA was generated using a Verso cDNA synthesis kit (Thermo Fisher). Real-time PCR was performed using StepOnePlus™ real-time PCR system (Applied Biosystems, Cheshire, UK) and the *Power* SYBR Green PCR Master Mix (Applied Biosystems). The PCR conditions were: 95°C for 10 min, followed by 40 cycles of 95°C for 15 s and 60°C for 1 min. Each PCR experiment was performed in triplicate. Transcript levels were normalized by *Hprt* expression levels.

QUANTIFICATION AND STATISTICAL ANALYSIS

Statistical details of experiments, such as exact value of n, what n represents, precision measures (means ± SEM), and statistical significance can be found in the figure legends. Statistical analysis was performed using Excel (Microsoft). Statistical significance was defined as $p < 0.05$. A two-tailed Student t test was performed on control versus experimental samples. Analysis of variance was used to test the difference in assesing the effects of shRNA against *Pafah1b1*(Figure 2A).